IET Intelligent Transport Systems

Special Issue: AI Applications to Intelligent Vehicles for Advancing Intelligent Transport Systems

IET Journals
The Institution of Engineering and Technology

Gaussian learning-based fuzzy predictive cruise control for improving safety and economy of connected vehicles

ISSN 1751-956X
Received on 7th July 2019
Revised 4th October 2019
Accepted on 11th February 2020
E-First on 19th March 2020
doi: 10.1049/iet-its.2019.0452
www.ietdl.org

Defeng He[1,2] ✉, *Binbin Peng*[1]

[1]*College of Information Engineering, Zhejiang University of Technology, Hangzhou 310023, People's Republic of China*
[2]*State Key Laboratory of Automotive Simulation and Control, Changchun 130025, People's Republic of China*
✉ *E-mail: hdfzj@zjut.edu.cn*

Abstract: This study considers an adaptive cruise control problem of connected vehicles in the vehicular *ad-hoc* network and proposes a Gaussian learning-based fuzzy predictive cruise control approach to enhance the fuel efficiency and safety of the connected vehicles in a vehicle-following scenario. First, a Gaussian process regression model is introduced and trained with real data to estimate the future acceleration of the preceding vehicle over the prediction horizon. Moreover, with assessing traffic scenarios, the weights characterising the importance of individual performance are adjusted by a fuzzy decision method in real time. Then a fuzzy predictive cruise controller is obtained by online solving a constrained receding horizon optimal control problem with a changing cost function and acceleration prediction of the preceding vehicle. Finally, through CarSim/Simulink co-simulation, it is shown that the proposed approach has an improvement in fuel economy and safety compared with conventional predictive cruise control algorithms.

1 Introduction

With the increasing road vehicles, the problems of road congestion, environmental pollution, energy consumption, and traffic safety become more and more serious. As an extension of traditional cruise control (CC), adaptive CC (ACC) can automatically adjust the vehicle speed by controlling throttle and braking units to improve the driving safety and ride comfort [1, 2]. Hence, ACC is an important technology of the advanced intelligent transportation system to reduce road congestion and improve fuel economy and driving safety.

The primary objectives of early ACC systems are to increase driving safety and comfort but not fuel economy. For example, Zhang and Ioannou [3] used a PID control algorithm to achieve a constant cruise speed of the host vehicle and safe inter-vehicle distances. With the rich studies on ACC systems, more objectives are hoped to be achieved except the early ones, such as fuel efficiency, emission, and comfort [4–6]. Model predictive control (MPC) has advantages to explicitly cope with constraints and multi-objective control has been widely used in the design of ACC systems in recent years. For example, a weight-free multi-objective predictive cruise control approach was proposed for autonomous vehicles [7]. In [8, 9], the authors verified MPC-based ACC. Combined with yaw moment control, MPC was adopted to design the ACC upper controller for improving ride comfort in [10]. The authors of [11, 12] used MPC to coordinate comfort, fuel economy, safety and car-following of ACC. In [13], an enhanced MPC-based ACC controller was presented to improve tracking accuracy and fuel economy by using road elevation information, non-linear powertrain dynamics and spatiotemporal constraint from the preceding vehicle. By wireless communication, the real-time information of the preceding vehicle was used to design predictive cruise control (PCC) algorithms to reduce the sudden changes of the host vehicle's acceleration when switching the ACC system mode [14]. This PCC algorithm improved the ride comfort of the host vehicle.

In PCC, some weighted cost functions are used to compromise the objectives of ACC, such as tracking, fuel efficiency, safety, comfort, etc. The weights generally characterise the relative importance of the individual objective. A real-time varying weights policy has been shown to improve the cruise performance of ACC because the weights can be adjusted according to different traffic scenarios. In [15], the MPC method of adjusting the weights in real time was used to improve the fuel economy and ride comfort for the cut in or cut out the condition of the preceding vehicle. However, when the traditional MPC deals with the preceding vehicle's acceleration disturbance of ACC models, it is assumed that the disturbance over the prediction horizon is constant. Since the acceleration of the preceding vehicle is generally uncertain and unknown, the performance of PCC may be poor if the acceleration of the preceding vehicle changes continuously. To solve this problem, Mesbah [16] adopted a closed-loop control strategy to compensate for the influence of the acceleration disturbance of the preceding vehicle.

Alternatively, since the acceleration or speed profile of the preceding vehicle is a kind of time-series data, it can be estimated using data learning methods. For instance, Jing *et al.* [17] used a cooperative Markov-AR method to predict the speed profile of vehicles. In [18, 19] Markov models were used to predict the traffic flow speed. The authors in [20] developed a short-term speed prediction algorithm by an artificial neural network. In [21] some widely used parameterised and non-parametric methods were compared based on the prediction of time series data, which showed that the Gaussian process could describe the acceleration or speed profile of the preceding vehicle. The authors in [22] systematically described the Gaussian process regression method. In [23] a conditional linear Gaussian model was adopted to predict the longitudinal velocity of the preceding vehicle. Moreover, a Gaussian process prediction was improved by integrating vehicle speed and traffic flow speed time-series data obtained from a cloud service as additional input for the Gaussian process [24]. In addition, the car-following and ride comfort performances for different traffic scenarios will be different during the driving process. A set of fixed weights is difficult to adapt to meet complex and changing traffic scenarios. The appropriate weights should be chosen according to the different scenarios. Since the fuzzy decision can design the corresponding control law based on a large number of artificial experiences and rules [25, 26], it can be used to adjust the weights of PCC according to the different scenarios.

In this paper, we consider the adaptive cruise control problem of connected vehicles in the vehicular *ad-hoc* network and propose a Gaussian learning-based fuzzy predictive cruise control approach to enhance fuel efficiency and safety in a vehicle-following scenario of the connected vehicles. The Gaussian process

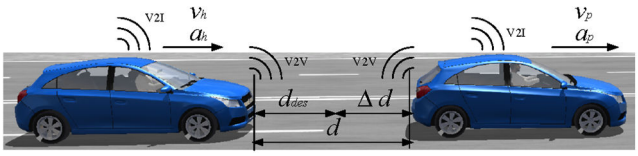

Fig. 1 *Schematic diagram of the vehicle tracking scenario*

regression model is introduced and trained with real data to estimate the external disturbance of the host vehicular ACC system, i.e. the future acceleration of the preceding vehicle over the prediction horizon. Moreover, the weights of the compromised cost function in PCC are real-time adjusted by the fuzzy decision method based on the assessment of the traffic scenarios and the current traffic scenario. Then the proposed predictive cruise controller is computed by online solving a constrained moving horizon optimal control problem with a changing weighted cost function and an acceleration prediction of the preceding vehicle. Finally, the proposed approach is evaluated and compared with the standard predictive cruise control algorithms by CarSim/Simulink co-simulation. The simulation results demonstrate that the proposed approach owns a significant improvement in fuel economy and safety compared with the standard PCC.

The remaining part of this paper is organised as follows: The PCC problem is described in Section 2. In Section 3, the Gaussian process regression method is introduced to predict the acceleration of the preceding vehicle. Section 4 designs the Gaussian learning-based PCC algorithm with fixed weights and Section 5 presents the Gaussian learning-based fuzzy PCC algorithm with varying weights. In Section 6, the comparative results are analysed between the proposed PCC and the traditional PCC. Section 7 concludes the paper.

2 Problem description

Consider a vehicle tracking scenario on a single lane, as shown in Fig. 1, where d is the inter-vehicle distance (i.e. spacing) between the host vehicle and its predecessor, v_i and a_i are the velocity and acceleration of the ith vehicle, respectively, $i = h$ denotes the host vehicle and $i = p$ denotes the preceding vehicle. The host vehicle is equipped with ACC to follow its predecessor. By V2V and V2I wireless communication, a_p will be real-time transmitted to the host vehicle to improve the assessment of the current traffic situation. Here the wireless communication is assumed to be ideal without time delays and packet loss. Moreover, lane changing and vehicles that are exiting or joining the string are outside the scope of this paper.

Due to non-linear dynamics of engine and drive train, aerodynamic drag, and rolling resistance, here a following linearised third-order model is employed to describe the longitudinal dynamics of the host vehicle:

$$\begin{aligned} \dot{x}_h(t) &= v_h(t), \\ \dot{v}_h(t) &= a_h(t), \\ \dot{a}_h(t) &= -1/\tau_d a_h(t) + 1/\tau_d a_{\text{des}}(t), \end{aligned} \tag{1}$$

where x_h is the absolute position of the host vehicle, τ_d is a constant time representing the internal actuator dynamics, and a_{des} is the desired acceleration command of the host vehicle. This model is widely used to design the upper controller of the longitudinal ACC system by assuming that the commanded acceleration can be exactly followed by the lower engine controlled in ECU of vehicles [8]. In this paper, we concentrate on the upper controller of the longitudinal ACC system. Moreover, the actuation delay between the real acceleration and the commanded acceleration is not considered here.

The basic objective of ACC is to follow its preceding vehicle at a desired spacing d_{des}. We use the constant time-headway spacing policy to define d_{des}, i.e. $d_{\text{des}}(t) = t_h v_h(t) + d_0$, where t_h is the headway time and d_0 is a safety spacing at a standstill. Then the spacing error with respect to d_{des} is computed as $\Delta d(t) = d(t) - d_{\text{des}}(t) = x_p(t) - x_h(t) - L_h - d_{\text{des}}(t)$ with the length of the preceding vehicle L_h.

Let the state vector $\boldsymbol{x} = [\Delta d \; \Delta v \; a_h]^{\text{T}}$ with $\Delta v = v_p - v_h$ and the control input $u = a_{\text{des}}$. From (1), the state-space model of the ACC system is represented by

$$\begin{aligned} \dot{\boldsymbol{x}}(t) &= \boldsymbol{A}\boldsymbol{x}(t) + \boldsymbol{B}u(t) + \boldsymbol{G}w(t), \\ \boldsymbol{y}(t) &= \boldsymbol{C}\boldsymbol{x}(t), \end{aligned} \tag{2}$$

where the external input w is the acceleration a_p of the preceding vehicle, the system output $\boldsymbol{y} = \boldsymbol{x}$, and matrices

$$\begin{aligned} \boldsymbol{A} &= \begin{bmatrix} 0 & 1 & -t_h \\ 0 & 0 & -1 \\ 0 & 0 & -1/\tau_d \end{bmatrix}, \quad \boldsymbol{B} = \begin{bmatrix} 0 \\ 0 \\ 1/\tau_d \end{bmatrix} \\ \boldsymbol{G} &= [0 \quad 1 \quad 0]^{\text{T}}, \qquad \boldsymbol{C} = \text{diag}\{1, 1, 1\} \end{aligned} \tag{3}$$

In order to adopt MPC to design ACC of the host vehicle, the ACC system (2) is discretised with a sampling time T as

$$\begin{aligned} \boldsymbol{x}(k+1) &= \boldsymbol{A}_k\boldsymbol{x}(k) + \boldsymbol{B}_k u(k) + \boldsymbol{G}_k w(k) \\ \boldsymbol{y}(k) &= \boldsymbol{C}_k\boldsymbol{x}(k) \end{aligned} \tag{4}$$

with the coefficient matrices

$$\begin{aligned} \boldsymbol{A}_k &= \begin{bmatrix} 1 & T & -t_h T \\ 0 & 1 & -T \\ 0 & 0 & 1 - T/\tau_d \end{bmatrix}, \quad \boldsymbol{B}_k = \begin{bmatrix} 0 \\ 0 \\ T/\tau_d \end{bmatrix} \\ \boldsymbol{G}_k &= [0 \quad T \quad 0]^{\text{T}}, \qquad \boldsymbol{C}_k = \text{diag}\{1, 1, 1\} \end{aligned} \tag{5}$$

where k is the sampling instant.

Besides the tracking objective of ACC, we consider fuel efficiency and safety in a vehicle-following scenario. To this end, a weighted cost function is often used to compromise these objectives of ACC in the framework of receding horizon MPC. It is clear that in MPC, the controller is only computed if the external input, i.e. the acceleration of the predecessor, is known over the prediction horizon. In practice, however, the acceleration of the preceding vehicle cannot be obtained over the prediction horizon except via V2X wireless communication at the current time. Since the external input is uncertain, the predicted errors over the horizon can be large in the worst case, which degrades the obtained control performance. Alternatively, data-driven learning approaches, e.g. the Gaussian process regression method, can be introduced to forecast the acceleration of the preceding vehicle over the prediction horizon. Hence, the controller has a better performance than conventional ones with omitting or invariant external input. To further improve the performance of ACC, the weights in the cost function of the controller have to be varying according to the assessment of the traffic situation over the prediction horizon. A practical solution for this problem is the fuzzy approach, which is well suited for this application.

3 Gaussian learning-based acceleration prediction of preceding vehicles

The acceleration $a_p(k-p),\ldots,a_p(k-1)$ at the p historical instants $(k-p),\ldots,(k-1)$ of the preceding vehicle is measured at time k. Let

$$\begin{aligned} \boldsymbol{K} &= [k_1 \quad k_2 \quad \cdots \quad k_p]^{\text{T}} \\ &= [k-p \quad k-p+1 \quad \cdots \quad k-1]^{\text{T}}, \\ \boldsymbol{A}_p &= [a_{p1} \quad a_{p2} \quad \cdots \quad a_{pp}]^{\text{T}} \\ &= [a_p(k-p) \quad a_p(k-p+1) \quad \cdots \quad a_p(k-1)]^{\text{T}} \end{aligned} \tag{6}$$

At this time, $\boldsymbol{K}$ and $\boldsymbol{A}_p$ are regarded as the input and output of the training set. Each value in the $\boldsymbol{A}_p$ can be regarded as a random

variable, which assumed that each variable in $\boldsymbol{A}_p$ obeys a Gaussian distribution, and all elements in the $\boldsymbol{A}_p$ obey the joint Gaussian distribution [24], i.e.

$$\boldsymbol{A}_p = \boldsymbol{F}(\boldsymbol{K}, \boldsymbol{K}) \sim \boldsymbol{N}(\boldsymbol{\mu}(\boldsymbol{K}, \boldsymbol{K}), \boldsymbol{\sigma}(\boldsymbol{K}, \boldsymbol{K})) \tag{7}$$

where $\boldsymbol{\mu}(\boldsymbol{K}, \boldsymbol{K})$ is the mean matrix of $\boldsymbol{F}(\boldsymbol{K}, \boldsymbol{K})$ and is set to be a zero matrix, $\boldsymbol{\sigma}(\boldsymbol{K}, \boldsymbol{K})$ is the covariance matrix of $\boldsymbol{F}(\boldsymbol{K}, \boldsymbol{K})$, which can be calculated by the covariance function $m(k_a, k_b)$, $k_a, k_b \in \boldsymbol{K}$, the covariance function $m(k_a, k_b)$ chooses the square exponential function type, i.e.

$$m(k_a, k_b) = \left[\sigma_f^2 \exp\left[\frac{-(k_a - k_b)^2}{2l^2}\right]\right] \tag{8}$$

where σ_f^2 is the sample variance and l is the variance scale.

Next, we calculate the covariance matrix $\boldsymbol{\sigma}(\boldsymbol{K}, \boldsymbol{K})$ of the training set input sample K, i.e.

$$\boldsymbol{\sigma}(\boldsymbol{K}, \boldsymbol{K}) = \begin{bmatrix} m(k_1, k_1) & m(k_1, k_2) & \cdots & m(k_1, k_p) \\ m(k_2, k_1) & m(k_2, k_2) & \cdots & m(k_2, k_p) \\ \vdots & \vdots & \ddots & \vdots \\ m(k_p, k_1) & m(k_p, k_2) & \cdots & m(k_p, k_p) \end{bmatrix} \tag{9}$$

Let the parameter $\theta = (\sigma_f^2, l)$ and calculate the log-likelihood function $L(\theta)$, i.e.

$$\begin{aligned} L(\theta) = & -\frac{1}{2} A_p^{\mathrm{T}} \boldsymbol{\sigma}(\boldsymbol{K}, \boldsymbol{K})^{-1} A_p \\ & -\frac{1}{2} \log|\boldsymbol{\sigma}(\boldsymbol{K}, \boldsymbol{K})| - \frac{p}{2} \log 2\pi \end{aligned} \tag{10}$$

Equation (10) is a non-convex optimisation problem. The Newton method and the conjugate gradient method can be used to obtain the optimal value of θ [27, 28].

The acceleration $a_p^*(k+1), \ldots, a_p^*(k+p)$ in the p future instants $(k+1), \ldots, (k+p)$ of the preceding vehicle is measured at time k. Let $\boldsymbol{K}^* = [k_1^*, \ldots, k_p^*]^{\mathrm{T}} = [k+1, \ldots, k+p]^{\mathrm{T}}$ and

$$\boldsymbol{A}_p^* = [a_{p1}^*, \ldots, a_{pp}^*]^{\mathrm{T}} = [a_p^*(k+1), \ldots, a_p^*(k+p)]^{\mathrm{T}} \tag{11}$$

At this time, $\boldsymbol{K}^*$ are regarded as the input to test set to predict the values of $\boldsymbol{A}_p^*$. Each value in the $\boldsymbol{A}_p^*$ can be regarded as a random variable, which assumed that each variable in $\boldsymbol{A}_p^*$ obeys a Gaussian distribution, and all elements in the $\boldsymbol{A}_p^*$ obey the joint Gaussian distribution [24], i.e.

$$\boldsymbol{A}_p^* = \boldsymbol{F}(\boldsymbol{K}^*, \boldsymbol{K}^*) \sim \boldsymbol{N}(\boldsymbol{\mu}(\boldsymbol{K}^*, \boldsymbol{K}^*), \boldsymbol{\sigma}(\boldsymbol{K}^*, \boldsymbol{K}^*)) \tag{12}$$

where $\boldsymbol{\mu}(\boldsymbol{K}^*, \boldsymbol{K}^*)$ is the mean matrix of $\boldsymbol{F}(\boldsymbol{K}^*, \boldsymbol{K}^*)$, where $\boldsymbol{\mu}(\boldsymbol{K}^*, \boldsymbol{K}^*)$ is set as zero matrix. $\boldsymbol{\sigma}(\boldsymbol{K}^*, \boldsymbol{K}^*)$ is the covariance matrix of $\boldsymbol{F}(\boldsymbol{K}^*, \boldsymbol{K}^*)$, which can be calculated by the covariance function $m(k_a^*, k_b^*)$, $k_a^*, k_b^* \in \boldsymbol{K}^*$. With free of noise, the training set output $\boldsymbol{F}(\boldsymbol{K}, \boldsymbol{K})$ and the test set output $\boldsymbol{F}(\boldsymbol{K}^*, \boldsymbol{K}^*)$ obey the following combined with Gaussian distribution:

$$\begin{bmatrix} \boldsymbol{F}(\boldsymbol{K}, \boldsymbol{K}) \\ \boldsymbol{F}(\boldsymbol{K}^*, \boldsymbol{K}^*) \end{bmatrix} \sim N\left(\boldsymbol{0}, \begin{bmatrix} \boldsymbol{\sigma}(\boldsymbol{K}, \boldsymbol{K}) & \boldsymbol{\sigma}(\boldsymbol{K}^*, \boldsymbol{K})^T \\ \boldsymbol{\sigma}(\boldsymbol{K}^*, \boldsymbol{K}) & \boldsymbol{\sigma}(\boldsymbol{K}^*, \boldsymbol{K}^*) \end{bmatrix}\right) \tag{13}$$

Next, we calculate the covariance matrix $\boldsymbol{\sigma}(\boldsymbol{K}^*, \boldsymbol{K}^*)$ of the test set input $\boldsymbol{K}^*$, i.e.

$$\boldsymbol{\sigma}(\boldsymbol{K}^*, \boldsymbol{K}^*) = \begin{bmatrix} m(k_1^*, k_1^*) & m(k_1^*, k_2^*) & \cdots & m(k_1^*, k_p^*) \\ m(k_2^*, k_1^*) & m(k_2^*, k_2^*) & \cdots & m(k_2^*, k_p^*) \\ \vdots & \vdots & \ddots & \vdots \\ m(k_p^*, k_1^*) & m(k_p^*, k_2^*) & \cdots & m(k_p^*, k_p^*) \end{bmatrix} \tag{14}$$

and calculate the covariance matrix $\boldsymbol{\sigma}(\boldsymbol{K}^*, \boldsymbol{K})$ of the test set input $\boldsymbol{K}^*$ and the training set input K, i.e.

$$\boldsymbol{\sigma}(\boldsymbol{K}^*, \boldsymbol{K}) = \begin{bmatrix} m(k_1^*, k_1) & m(k_1^*, k_2) & \cdots & m(k_1^*, k_p) \\ m(k_2^*, k_1) & m(k_2^*, k_2) & \cdots & m(k_2^*, k_p) \\ \vdots & \vdots & \ddots & \vdots \\ m(k_p^*, k_1) & m(k_p^*, k_2) & \cdots & m(k_p^*, k_p) \end{bmatrix} \tag{15}$$

Referring to (13) combined with Gaussian distribution, according to the Gaussian distribution property, the conditional distribution $\boldsymbol{F}(\boldsymbol{K}^*, \boldsymbol{K}^*)|F(\boldsymbol{K}, \boldsymbol{K})$ of $\boldsymbol{F}(\boldsymbol{K}^*, \boldsymbol{K}^*)$ can be obtained as

$$\begin{aligned} & \boldsymbol{F}(\boldsymbol{K}^*, \boldsymbol{K}^*) \,|\, \boldsymbol{F}(\boldsymbol{K}, \boldsymbol{K}) \\ & \quad \sim N\begin{pmatrix} \boldsymbol{\sigma}(K^*, K)\boldsymbol{\sigma}(K, K)^{-1} A_p, \\ \boldsymbol{\sigma}(K^*, K^*) - \boldsymbol{\sigma}(K^*, K)\boldsymbol{\sigma}(K, K)^{-1}\boldsymbol{\sigma}(K^*, K)^{\mathrm{T}} \end{pmatrix} \end{aligned} \tag{16}$$

Then, for the prediction of the acceleration $\boldsymbol{A}_p^*$ at the p future instants, the mean of the $\boldsymbol{F}(\boldsymbol{K}^*, \boldsymbol{K}^*)$ conditional distribution can be used as the $\boldsymbol{A}_p^*$ estimate, i.e.

$$\boldsymbol{A}_p^* = \boldsymbol{\sigma}(\boldsymbol{K}^*, \boldsymbol{K})\boldsymbol{\sigma}(\boldsymbol{K}, \boldsymbol{K})^{-1} \boldsymbol{A}_p \tag{17}$$

At the next moment $\boldsymbol{K}+1$, the acceleration value of the p-time of the new history of the preceding vehicle is re-measured, and the above steps are repeated. The acceleration value of the preceding vehicle at the new future p instants can be predicted at the next instant, and we take the first predicted value as the reference value of the next time. In this way, the acceleration value of the preceding vehicle can be predicted online and the deviation of prediction can be corrected continuously.

4 Gaussian learning-based PCC algorithms with fixed weights

The vehicle-following kinematics model (4) and (5) is used as the prediction model to predict the future action of the PCC system by p-step. The p-step prediction output vector and the p-step input vector are defined as

$$\begin{aligned} \boldsymbol{Y}_p^*(k) &= \begin{bmatrix} y^*(k+1) & y^*(k+2) & \cdots & y^*(k+p) \end{bmatrix}^{\mathrm{T}} \\ \boldsymbol{U}(k) &= \begin{bmatrix} u(k) & u(k+1) & \cdots & u(k+p) \end{bmatrix}^{\mathrm{T}} \end{aligned} \tag{18}$$

Considering the preceding vehicle acceleration disturbance predicted by the Gaussian process regression model, the p-step acceleration disturbance values are defined as

$$\boldsymbol{W}^* = \begin{bmatrix} w^*(k) & w^*(k+1) & \cdots & w^*(k+p) \end{bmatrix}^{\mathrm{T}} \tag{19}$$

Then, the output of the future p-step prediction of the system can be expressed as

$$\boldsymbol{Y}_p^*(k) = \boldsymbol{S}_x \boldsymbol{x}(k) + \boldsymbol{S}_u \boldsymbol{U}(k) + \boldsymbol{S}_d \boldsymbol{W}^* \tag{20}$$

Combining (11) and (17) for further development

$$\begin{aligned} \boldsymbol{Y}_p^*(k) &= \boldsymbol{S}_x \boldsymbol{x}(k) + \boldsymbol{S}_u \boldsymbol{U}(k) + \boldsymbol{S}_d \boldsymbol{A}_p^* \\ &= \boldsymbol{S}_x \boldsymbol{x}(k) + \boldsymbol{S}_u \boldsymbol{U}(k) + \boldsymbol{S}_d \boldsymbol{\sigma}(\boldsymbol{K}^*, \boldsymbol{K})\boldsymbol{\sigma}(\boldsymbol{K}, \boldsymbol{K})^{-1} \boldsymbol{A}_p \end{aligned} \tag{21}$$

where the matrices

$$
\begin{aligned}
\boldsymbol{S}_x &= \left[(\boldsymbol{C}_k\boldsymbol{A}_k)^{\mathrm{T}} \quad (\boldsymbol{C}_k\boldsymbol{A}_k^2)^{\mathrm{T}} \quad \cdots \quad (\boldsymbol{C}_k\boldsymbol{A}_k^p)^{\mathrm{T}}\right]^{\mathrm{T}}_{1\times p} \\
\boldsymbol{S}_d &= \begin{bmatrix} \boldsymbol{C}_k\boldsymbol{G}_k & 0 & \cdots & 0 \\ \boldsymbol{C}_k\boldsymbol{A}_k\boldsymbol{G}_k & \boldsymbol{C}_k\boldsymbol{G}_k & \cdots & 0 \\ \vdots & \vdots & \ddots & \vdots \\ \boldsymbol{C}_k\boldsymbol{A}_k^{p-1}\boldsymbol{G}_k & \boldsymbol{C}_k\boldsymbol{A}_k^{p-2}\boldsymbol{G}_k & \cdots & \boldsymbol{C}_k\boldsymbol{G}_k \end{bmatrix}_{p\times p} \\
\boldsymbol{S}_u &= \begin{bmatrix} \boldsymbol{C}_k\boldsymbol{B}_k & 0 & \cdots & 0 \\ \boldsymbol{C}_k\boldsymbol{A}_k\boldsymbol{B}_k & \boldsymbol{C}_k\boldsymbol{B}_k & \cdots & 0 \\ \vdots & \vdots & \ddots & \vdots \\ \boldsymbol{C}_k\boldsymbol{A}_k^{p-1}\boldsymbol{B}_k & \boldsymbol{C}_k\boldsymbol{A}_k^{p-2}\boldsymbol{B}_k & \cdots & \boldsymbol{C}_k\boldsymbol{B}_k \end{bmatrix}_{p\times p}
\end{aligned} \tag{22}
$$

In the steady-state vehicle following conditions, the expected vehicle spacing error Δd, the relative speed Δv tends to zero at the same time, the host vehicle acceleration can keep up with the preceding vehicle acceleration. Moreover, since the accelerating actions of vehicles do consume the fuel of vehicles, it is necessary to introduce some weights to punish the control input (i.e. the acceleration command) of the vehicular ACC system over the prediction steps. Therefore, the optimisation goal can be written as a weighted form of the value function [18]

$$
\begin{aligned}
J(k) &= \sum_{j=1}^{p} y^*(k+j)^{\mathrm{T}}\boldsymbol{Q}y^*(k+j) + u(k+j)^{\mathrm{T}}\boldsymbol{R}u(k+j) \\
&= \boldsymbol{Y}_p^*(k)^T\bar{\boldsymbol{Q}}\boldsymbol{Y}_p^*(k) + \boldsymbol{U}(k)^T\bar{\boldsymbol{R}}\boldsymbol{U}(k)
\end{aligned} \tag{23}
$$

where $\boldsymbol{Q}$ is the positive-definite matrix punishing the system output and weight $R>0$ punishes the control actions to lessen the acceleration command of the host vehicle. In general, $\boldsymbol{Q}$ is selected to be a diagonal matrix $\boldsymbol{Q}=\mathrm{diag}\{q_1, q_2, q_3\}$ with $q_i>0$ for $i=1, 2, 3$. Elaborately tuning of $\boldsymbol{Q}$ and $\boldsymbol{R}$ may improve the satisfactory cruising performance of the ACC controller.

To improve ride comfort as well as satisfying the physical characteristics of the host vehicle, the range of the acceleration command of the vehicular ACC systems is subject to the following constraint:

$$
u_{\min} \le u \le u_{\max} \tag{24}
$$

In order to facilitate the minimisation of $J(k)$, (23) is equal to the form of quadratic programming and defined

$$
\boldsymbol{E}(k) = -(\boldsymbol{S}_x\boldsymbol{x}(k) + \boldsymbol{S}_d\boldsymbol{A}_p^*) \tag{25}
$$

where $\boldsymbol{E}(k)$ is independent of the amount of control, then (23) can be transformed as follows:

$$
\begin{aligned}
J(k) &= \| \bar{\boldsymbol{Q}}(\boldsymbol{S}_u\boldsymbol{U}(k) - \boldsymbol{E}(k)) \|^2 + \| \boldsymbol{R}\boldsymbol{U}(k) \|^2 \\
&= \boldsymbol{U}(k)^{\mathrm{T}}\boldsymbol{S}_u^{\mathrm{T}}\bar{\boldsymbol{Q}}^{\mathrm{T}}\bar{\boldsymbol{Q}}\boldsymbol{S}_u\boldsymbol{U}(k) + \boldsymbol{U}(k)^{\mathrm{T}}\bar{\boldsymbol{R}}^{\mathrm{T}}\bar{\boldsymbol{R}}\boldsymbol{U}(k) \\
&\quad -2\boldsymbol{E}(k)\bar{\boldsymbol{Q}}^{\mathrm{T}}\bar{\boldsymbol{Q}}\boldsymbol{S}_u\boldsymbol{U}(k) + \boldsymbol{E}(k)^{\mathrm{T}}\bar{\boldsymbol{Q}}^{\mathrm{T}}\bar{\boldsymbol{Q}}\boldsymbol{E}(k)
\end{aligned} \tag{26}
$$

Ignore the amount unrelated to the amount of control, and define

$$
\boldsymbol{G}(k) = -2\boldsymbol{S}_u^{\mathrm{T}}\bar{\boldsymbol{Q}}^{\mathrm{T}}\bar{\boldsymbol{Q}}\boldsymbol{E}(k),\ \boldsymbol{H}(k) = \boldsymbol{S}_u^{\mathrm{T}}\bar{\boldsymbol{Q}}^{\mathrm{T}}\bar{\boldsymbol{Q}}\boldsymbol{S}_u + \bar{\boldsymbol{R}}^{\mathrm{T}}\bar{\boldsymbol{R}} \tag{27}
$$

Then formula (26) can be converted into

$$
J(k) = \boldsymbol{U}^{\mathrm{T}}(k)\boldsymbol{H}\boldsymbol{U}(k) + \boldsymbol{G}(k)\boldsymbol{U}(k) \tag{28}
$$

In addition, considering the constraint conditions of the vehicle when formula (24) is given, the control constraints are rewritten as

$$
\boldsymbol{C}_r\boldsymbol{U}(k) \le \boldsymbol{B}_r \tag{29}
$$

The coefficient matrices $\boldsymbol{C}_r$ and $\boldsymbol{B}_r$ are

$$
\boldsymbol{C}_r = \begin{bmatrix} -I \\ I \end{bmatrix},\quad \boldsymbol{B}_r = \begin{bmatrix} -U_{\min} \\ U_{\max} \end{bmatrix},\quad \boldsymbol{I} = \mathrm{diag}\{1, 1, \ldots, 1\} \tag{30}
$$

At this time, the optimisation problem in the adaptive cruise control system can be written as

$$
\begin{aligned}
&\min_{U(k)} J(k) = \boldsymbol{U}(k)^{\mathrm{T}}\boldsymbol{H}\boldsymbol{U}(k) + \boldsymbol{G}(k)\boldsymbol{U}(k) \\
&\text{s.t.} \quad \boldsymbol{G}(k) = -2\boldsymbol{S}_u^{\mathrm{T}}\bar{\boldsymbol{Q}}^{\mathrm{T}}\bar{\boldsymbol{Q}}\boldsymbol{E}(k) \\
&\qquad \boldsymbol{H}(k) = \boldsymbol{S}_u^{\mathrm{T}}\bar{\boldsymbol{Q}}^{\mathrm{T}}\bar{\boldsymbol{Q}}\boldsymbol{S}_u + \bar{\boldsymbol{R}}^{\mathrm{T}}\bar{\boldsymbol{R}} \\
&\qquad \boldsymbol{E}(k) = -(\boldsymbol{S}_x\boldsymbol{x}(k) + \boldsymbol{S}_d\boldsymbol{A}_p^*) \\
&\qquad \boldsymbol{A}_p^* = \boldsymbol{\sigma}(\boldsymbol{K}^*, \boldsymbol{K}^*)\sigma(\boldsymbol{K}, \boldsymbol{K})^{-1}\boldsymbol{A}_p \\
&\qquad \boldsymbol{C}_r\boldsymbol{U}(k) \le \boldsymbol{B}_r
\end{aligned} \tag{31}
$$

Note the minimisation problem (31) is identical to be a quadratic programming one. Therefore, the available numerical algorithms of quadratic programming can be used to solve the minimisation problem [29, 30], e.g. multiplier methods, SQP, etc.

5 Gaussian learning-based fuzzy PCC algorithms with varying weights

5.1 Adaptive adjustment of weighted coefficients

In consideration of different driving scenarios, different directions are emphasised for the vehicle following the performance and comfort performance of the host vehicle. The controller designed above adopts a fixed value form for the system output weighted matrix $\boldsymbol{Q}$ and the weighted matrix $\boldsymbol{R}$ of the control quantity of the system, which is difficult to adapt to the complex and changeable traffic environment. In order to make the host vehicle adaptively adjust the weights of the vehicle following and comfort weights in different driving environments, the host vehicle must meet the requirements for following performance and comfort performance during driving, and improve the adaptability of the ACC system to the environment. In this paper, a fuzzy decision is used to design the output weighted matrix $\boldsymbol{Q}$ and control weighted matrix $\boldsymbol{R}$ for dynamic adjustment of weighted coefficients. Note that the fuzzy membership functions used here are set as the form of trigonometric functions and the fuzzy rules and membership functions are designed according to the actual traffic scene as well as some trial-and-error experiments.

5.2 Fuzzification

Firstly, the fuzzy control input vehicle spacing error Δd, relative speed Δv, is blurred into five sets: NB (negative big), NS (negative small), ZO (zero), PS (positive small), PB (positive big), the variation range of Δd is set to $[-60, 80]$ m, the variation range of Δv is set to $[-20, 20]$ m/s, and the fuzzy control output vehicle spacing error weight q_1, relative velocity weight q_2. The relative acceleration weight q_3 is blurred into five sets VS (very small), S (small), M (medium), B (big). Because the weights (q_1, q_2, q_3) and comfort performance weight $\boldsymbol{R}$ have the relative sense, where the fixed weight $\boldsymbol{R}$ is 5 and the vehicle following performance weights (q_1, q_2, q_3) are taken as [0, 10]; the membership functions of each variable input and output are shown in Figs. 2–4 and Figs. 5 and 6, respectively.

5.3 Establishment of fuzzy rules

According to the actual traffic scene analysis, e.g. when the vehicle spacing error is in the NB (negative big) domain, it indicates that the situation is more critical and it is prone to rear-end collision. At this time, the vehicle spacing error weight and the relative velocity weight should be in the big domain (B), the relative acceleration weight is in a very small domain (VS) to ensure rapid deceleration of the host vehicle. When the relative velocity increases, the vehicle spacing error decreases, and the vehicle spacing error weight and relative speed weight decrease, the relative acceleration

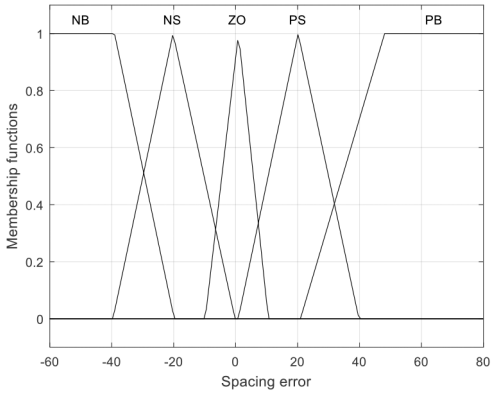

Fig. 2 *Membership function of the pitch error*

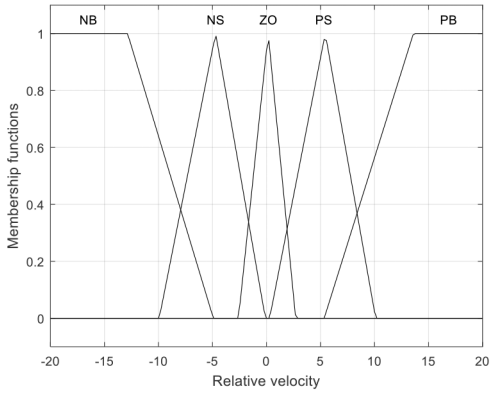

Fig. 3 *Membership function of relative velocity*

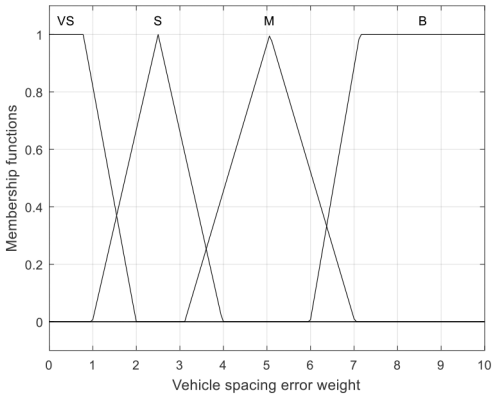

Fig. 4 *Membership function of spacing error weights*

weight is constantly increasing. When the space error and relative velocity is in ZO (zero) domain, it is shown that the two vehicles are in a safety inter-vehicle distance, since the host vehicle in the relatively stable tracks the preceding vehicle at the same time, which can reduce the vehicle following performance demand, increase the demand of comfort performance, this can make the space error weight and relative velocity weight in small domain (S), and the relative acceleration weight in middle domain (M), and at the same time as the relative velocity increased, the relative velocity and relative distance weight increase. When the error of inter-vehicle distance is in PB (positive big) domain, it indicates that the distance between the two vehicles is large, and the distance between the two vehicles will be larger and larger with the increase of the relative velocity. Therefore, the weight of relative velocity and distance should be increased, and the weight of relative acceleration should be reduced, so as to improve the performance of the vehicle following. Based on the above analysis, the specific fuzzy control rules of fuzzy control input quantity inter-vehicle distance error and relative velocity regarding the weight of fuzzy control output quantity vehicle spacing error weight, relative

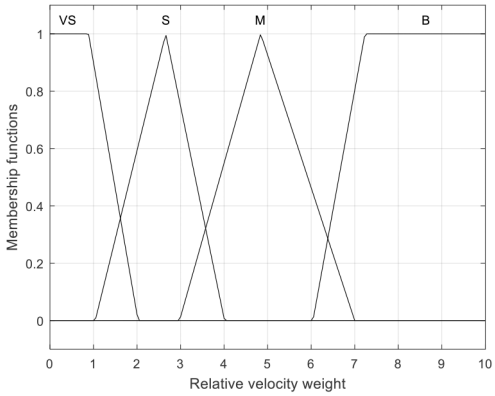

Fig. 5 *Membership function of relative velocity weights*

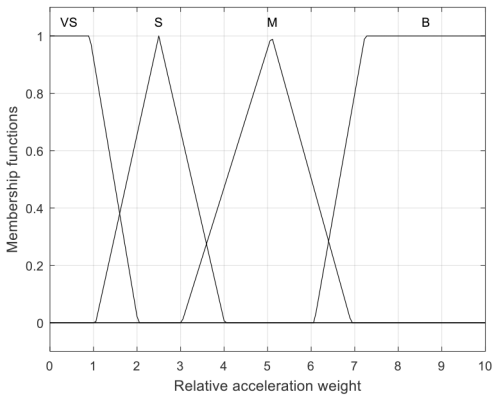

Fig. 6 *Membership function of relative acceleration weights*

velocity weight and relative acceleration weight are designed as Tables 1–3, respectively.

5.4 Anti-fuzzification

Defuzzification of fuzzy by the central method, and the obtained state quantities Δd and Δv are applied to the above-designed fuzzy controller at each moment, and the weight coefficients can be adjusted in real time according to different traffic scenarios, and then solving the optimisation problem of (25), we can get the control sequence $u(k)$, and the first solution of $u(k)$ is applied to the system. By using the characteristics of the rolling optimisation of the MPC algorithm, the control of the adaptive cruise system can be realised by repeating the above process at the next moment.

6 Simulation and results discussion

The vehicle model and simulation conditions are built-in CarSim software and the control system model is built in Simulink. The host vehicle and the preceding vehicle are selected to be C-class hatchback sedan with the front-wheel-drive and the engine power of 125 kW. In this study, the speed of the preceding vehicle is set as $v_p(t) = v_0 + 9.7\sin(0.3t)$ m/s with the initial speed $v_0 = 15.3$ m/s, the initial speed of the host vehicle is set as $v_h = 13.9$ m/s and the initial inter-vehicle distance is 40 m. Moreover, select $t_h = 2$ s, $\tau_d = 0.2$, $p = 10$, $d_0 = 5$ m, $\boldsymbol{Q} = 2.5\boldsymbol{I}_3$, $R = 5$, $T = 0.1$ s, $u_{\min} = -5$ m/s^2, and $u_{\max} = 5$ m/s^2. It is noted that the preceding car's speed profile involves three representative scenarios, i.e. varying accelerating (0–7.5 s), varying and emerging decelerating (7.5–18.5 s) and almost uniform speed (18.5–30 s). See the solid lines in Figs. 7 and 8. These representative scenarios widely exist in the real traffic scenarios and hence, have been widely used to illustrate the effectiveness of PCC [1, 6–9].

Let GLFW-PCC and GLVW-PCC denote the Gaussian learning-based PCC with fixed weights and varying weights, respectively. The proposed PCC is then compared with traditional PCC (denoted as T-PCC). Figs. 7–9 show the simulation results obtained by applying the three PCC approaches, where the solid

Table 1 Fuzzy control rules for vehicle spacing error and relative velocity with respect to vehicle spacing error weight

$\Delta d/\Delta v$	NB	NS	ZO	PS	PB
NB	B	B	B	B	M
NS	M	M	M	M	S
ZO	M	S	S	S	VS
PS	M	M	M	M	M
PB	B	B	M	B	B

Table 2 Fuzzy control rules for vehicle spacing error and relative velocity with respect to relative velocity weight

$\Delta d/\Delta v$	NB	NS	ZO	PS	PB
NB	B	M	M	M	B
NS	B	M	S	M	B
ZO	B	M	S	M	M
PS	B	M	S	M	B
PB	M	S	VS	S	B

Table 3 Fuzzy control rules for vehicle spacing error and relative velocity with respect to relative acceleration weight

$\Delta d/\Delta v$	NB	NS	ZO	PS	PB
NB	VS	S	S	S	VS
NS	VS	S	M	S	VS
ZO	VS	S	M	S	S
PS	VS	S	M	S	VS
PB	S	M	B	M	VS

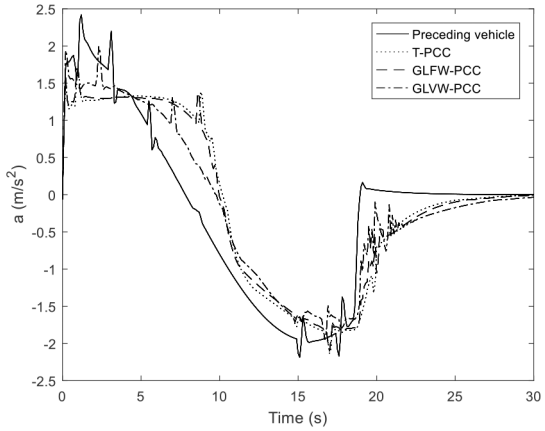

Fig. 7 *Acceleration in complex scenario*

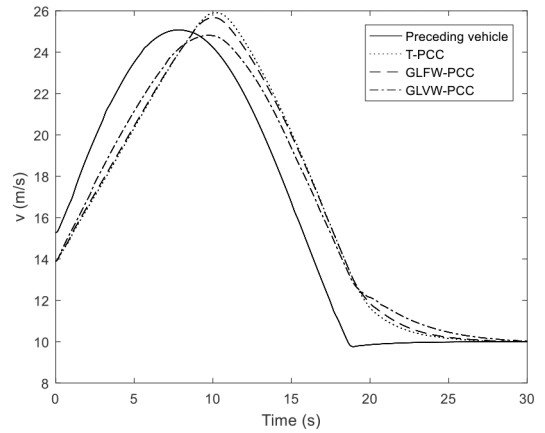

Fig. 8 *Velocity in complex scenario*

lines are associated with the preceding vehicle and the dotted, dashed, and dot-dashed lines are associated with T-PCC, GLFW-PCC and GLVW-PCC, respectively.

From Figs. 7–9, we can firstly see that the three PCC approaches can successfully avoid rear-end collision when the preceding car is driven with a varying velocity while satisfying the acceleration constraints. Furthermore, the responses of the cruise control systems with both GLFW-PCC and GLVW-PCC are faster than those with T-PCC regardless of when the preceding car is accelerating or decelerating. Taking the rapidly decelerating stage of the preceding car after 7.5 s for an example, T-PCC assumes that the deceleration value of the preceding vehicle is constant over the predictive horizon at each time. As a result, the control input computed by T-PCC does not quickly decelerate the host vehicle and generates a smaller inter-vehicle distance than those by applying GLFW-PCC and GLVW-PCC, which decreases the driving safety and ride comfort. Inversely, the inter-vehicle distance obtained by applying T-PCC is more than that by separately applying GLFW-PCC and GLVW-PCC when the preceding vehicle is accelerating from starting to 7.5 s, which decreases the capacity of road traffic. The main reason causing the difference between T-PCC and our learning-based PCC is that the acceleration/deceleration prediction of the preceding vehicle can be embedded into the optimisation control problem in GLFW-PCC and GLVW-PCC.

On the other hand, it is further observed from Figs. 7–9 that GLVW-PCC outperforms GLFW-PCC in terms of the responses of the closed-loop cruise control system of the host vehicle. Fig. 10 gives the changes in the weights in the optimisation problem (31) of GLVW-PCC. Compared with GLFW-PCC, GLVW-PCC uses larger weights of the relative velocity and acceleration at the initial time. Hence, the velocity by GLVW-PCC increases more quickly than that by GLFW-PCC, which better reduces the inter-vehicle distance and increases traffic capacity. When catching up with the preceding car, the host vehicle with GLVW-PCC is driven at a gentler speed than that with GLFW-PCC. This improves ride comfort and reduces fuel consumption. Using the GLVW-PCC method, the weighted coefficients of the performance function can be automatically adjusted to meet different driving scenarios.

Fig. 11 shows the accumulated fuel consumption over the total simulation time, where the dotted, dashed, and dot-dashed lines are associated with T-PCC, GLFW-PCC and GLVW-PCC, respectively. From Fig. 11, it can be seen that the host vehicle with GLVW-PCC consumes more accumulated fuel than that separately with GLFW-PCC and T-PCC when accelerating from starting to 7.5 s. This is caused by the fact that GLVW-PCC drives the host vehicle to follow the preceding car more quickly than the else (see Figs. 7–9). After 7.5 s, the host vehicle with GLVW-PCC consumes the smallest accumulated fuel than that with GLFW-PCC

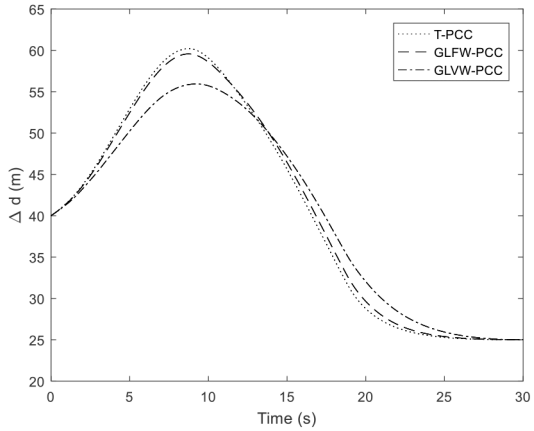

Fig. 9 *Inter-vehicle distance in complex scenario*

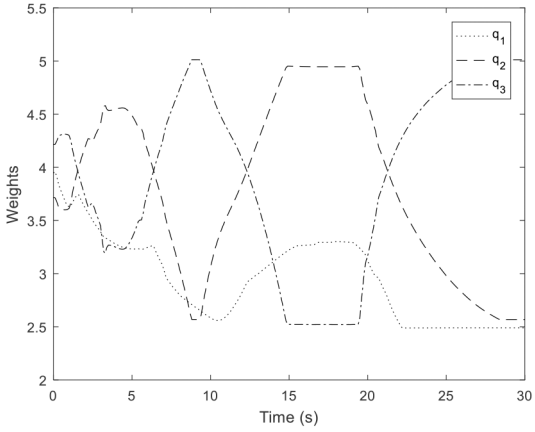

Fig. 10 *GLCW-PCC weight changes*

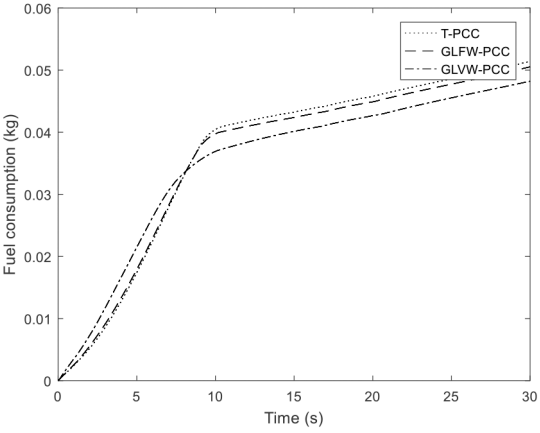

Fig. 11 *Accumulated fuel consumption in complex scenario*

Table 4 Fuel consumption by different PCC controllers

	T-PCC	GLFW-PCC	GLVW-PCC
fuel consumption, L/100 km	13.65	13.40	12.80
improvement, %	—	1.75	6.23

and T-PCC. Table 4 gives the fuel consumption in L/100 km of the host vehicle with the three PCC approaches and the improvement of the consumption with respect to T-PCC. One can see that compared with T-PCC, GLFW-PCC can reduce fuel consumption by 1.75% and GLVW-PCC can reduce fuel consumption by 6.23%. Note that the fuel economy improvements achieved here are also dependent on the elaborately tuning of weights $\boldsymbol{Q}$ and $\boldsymbol{R}$ in the cost function (23). In GLVW-PCC, the weights are adaptively updated by a fuzzy decision to accommodate the traffic scenarios forecasted by Gaussian process regression.

In what follows, we examine the effects of the prediction horizon p on the Gaussian process regression prediction and the computational time spent in one-time learning and online optimisation. Fig. 12 shows the comparison profiles of the real acceleration and predicted acceleration at different prediction steps, where solid lines are real-time acceleration profiles of the preceding vehicle and dash-dotted lines are the GLP-based predicted acceleration profiles. From Fig. 12, it is observed that the effect of the prediction step on the prediction accuracy is not monotonic. In order to further analyse the effects of the step on the prediction results, Table 5 lists the prediction accuracy and the average computational time of one-time learning and optimisation for different p. Here the average errors of the acceleration/deceleration prediction and the error variances are used to characterise the prediction accuracy of the Gaussian process regression prediction method. From the average prediction errors and the error variances in Table 5, one can see that the Gaussian process regression prediction method can effectively predict the acceleration changes of the preceding vehicle. It is further observed from Table 5 that the effect of p on the average prediction errors is not monotonic, but the effects on the error variances and average computational time are positive monotonically. Clearly, due to the uncertain driving scenarios, a longer horizon p may decrease the prediction accuracy [23]. Hence, the prediction step p is selected by making a trade-off between the prediction accuracy and average computational time of one-time learning and optimisation. Note that the computational time in Table 5 is to show the computational speed of the proposed method with the different prediction steps, but it does not mean the real-time computation speed when used in a real car, where MatLab is not used and the speed can be improved when low level language.

Finally, to illustrate the application of the proposed method, the three methods are further compared under the Worldwide Harmonized Light Vehicles Test Procedure (WLTP) condition [31]. The comparison results of the three methods are shown in Figs. 13–16, where the solid lines are associated with the preceding vehicle and the dotted, dashed, and dot-dashed lines are associated with T-PCC, GLFW-PCC and GLVW-PCC, respectively.

From Figs. 13–16, we can see that the three PCC approaches can successfully avoid rear-end collisions and satisfy the acceleration constraints when the preceding car is driven with a complex WLTP scenario. However, the driving behaviours of the host vehicle are different among the PCC methods. Take the 600–630 s for an example. In the case of fixed weights, although the acceleration of the preceding car is increasing, the T-PCC method still assumes that it does not change in the predictive horizon window. Hence, the predicted output of the PCC system is smaller and the computed acceleration command of the host vehicle is smaller than the others'. This suggests that the response of the cruise control systems with GLFW-PCC is faster than those with T-PCC and the spacing of the adjacent cars is also smaller than T-PCC's. On the other hand, compared with the fixed weight method, the variable weight PCC method uses larger weights on the relative velocity and relative acceleration at the initial time. Therefore, the velocity by GLVW-PCC increases faster than that by both GLFW-PCC and GLVW-PCC. Hence, it is beneficial to reduce the inter-vehicle distance and then to increase the traffic capacity of roads.

In addition, consider the period when catching up with the preceding vehicle. Due to the ride comfort performance, the host vehicle by GLVW-PCC approaches the preceding vehicle at a gentler speed than the vehicle by both GLFW-PCC and GLVW-PCC. This improves the ride comfort and reduces the fuel consumption of the host vehicle. Table 6 shows the fuel consumption of the host vehicle equipped with the three PCC controllers, respectively. From Table 6, it can be derived that the GLFW-PCC method can reduce fuel consumption by 0.42%, and the GLVW-PCC method can reduce fuel consumption by 0.62% compared with the T-PCC method. Note that these improvements are achieved by elaborately tuning the weights $\boldsymbol{Q}$ and $\boldsymbol{R}$ in (23), which in GLVW-PCC are adaptively adjusted by employing fuzzy decision and Gaussian process regression. These illustrate the application of the proposed PCC method.

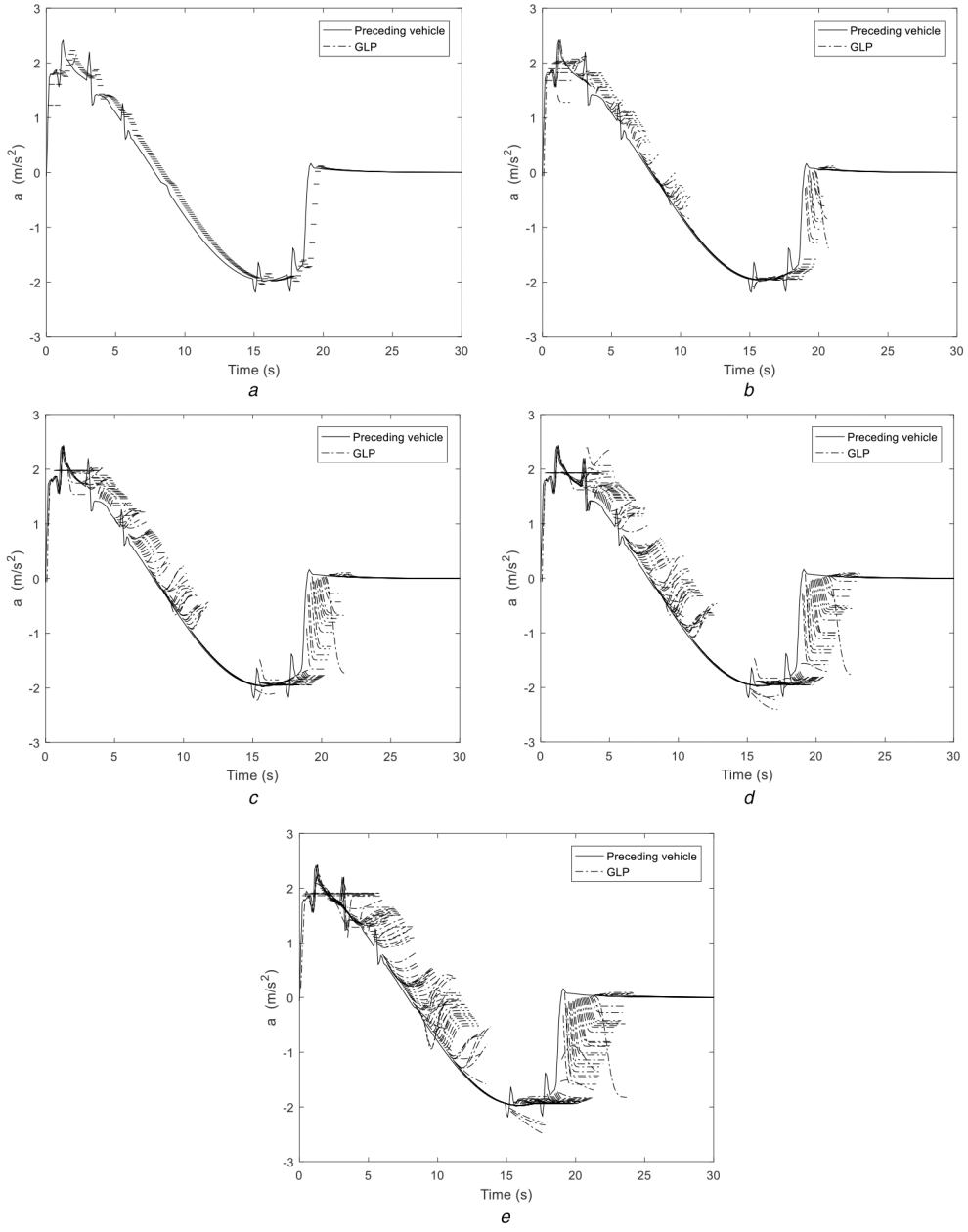

Fig. 12 *Acceleration comparisons at different prediction steps*
(a) $p = 5$, ***(b)*** $p = 10$, ***(c)*** $p = 15$, ***(d)*** $p = 20$, ***(e)*** $p = 25$

Table 5 Prediction accuracy and average computational time of one-time learning and optimisation for different p

p	Average errors	Error variances	Average time, ms
5	2.72×10^{-2}	0.2554	219
10	-8.9×10^{-3}	0.3326	235
15	4.5×10^{-3}	0.4393	261
20	6.9×10^{-3}	0.5367	276
25	-2.8×10^{-3}	0.6107	302

7 Conclusion

In this paper, a vehicle learning variable weight cruise controller based on Gaussian process regression is designed. The controller can effectively predict the acceleration of the preceding vehicle, and can adaptively adjust the performance index of the objective function according to different driving scenarios, thus improving the adaptability of vehicles to complex traffic environment. In addition, compared with the traditional model predictive cruise controller, the vehicle-following performance, vehicle safety, and fuel economy have been effectively improved. Finally, the fast computation and implementation of the proposed method are the subjects of ongoing work and in pursuing future work, engine efficiency and fuel consumption models will be used as the cost function of non-linear PCC.

8 Acknowledgments

The work was supported by the National Natural Science Foundation of China (61773345), Zhejiang Provincial Natural Science Foundation (LR17F030004) and Foundation of State Key Laboratory of Automotive Simulation and Control (20171103).

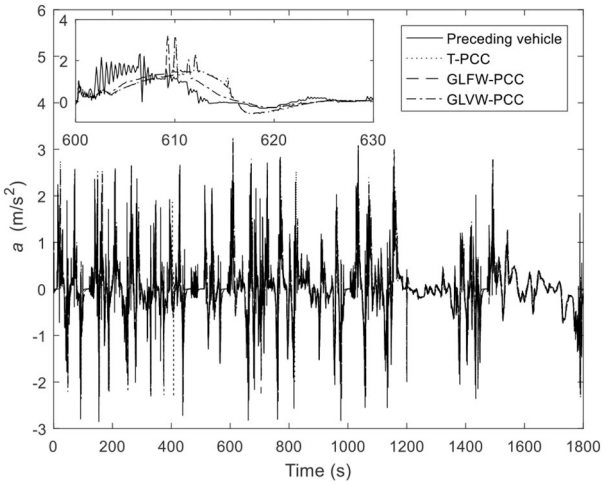

Fig. 13 *Acceleration in WLTP scenario*

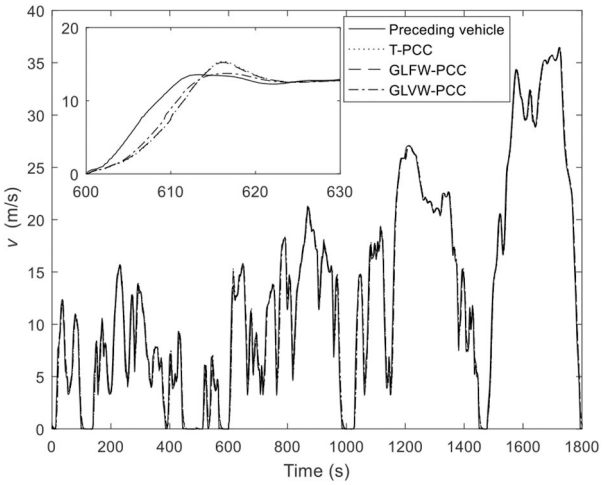

Fig. 14 *Velocity in WLTP scenario*

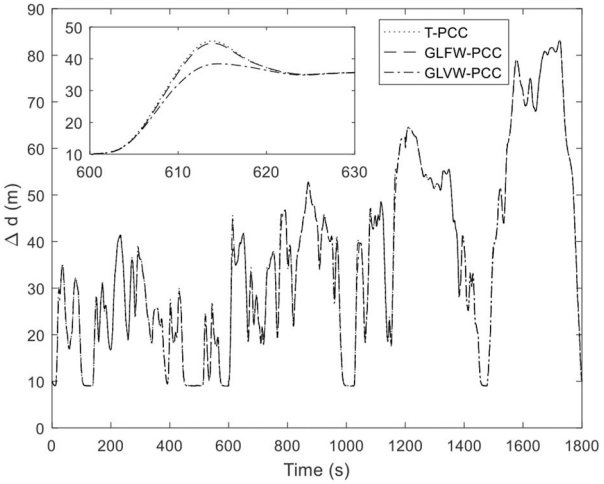

Fig. 15 *Inter-vehicle distance in WLTP scenario*

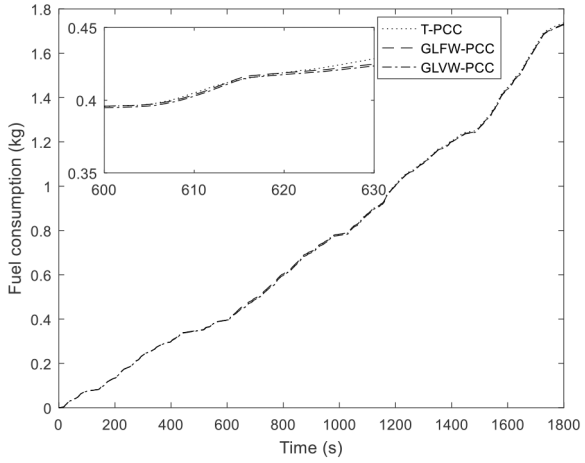

Fig. 16 *Accumulated fuel consumption in WLTP scenario*

Table 6 Fuel consumption by different PCC controllers for WLTP

	T-PCC	GLFW-PCC	GLVW-PCC
fuel consumption, L/100 km	9.62	9.58	9.56
improvement, %	—	0.42	0.62

9 References

[1] Li, S., Li, K., Rajamani, R., *et al.*: 'Model predictive multi-objective vehicular adaptive cruise control', *IEEE Trans. Control Syst. Technol.*, 2011, **19**, (3), pp. 556–566

[2] Wu, G., Zhang, L., Liu, Z., *et al.*: 'Research status and development trend of automobile adaptive cruise control system', *J. Tongji Univ.*, 2017, **45**, (4), pp. 544–553

[3] Zhang, J., Ioannou, P.A.: 'Control of heavy-duty trucks: environmental and fuel economy considerations', *IEEE Trans. Intell. Transp. Syst.*, 2006, **7**, (1), pp. 92–104

[4] He, D., Wang, L., Sun, J.: 'On stability of multi-objective NMPC with objective prioritization', *Automatica*, 2015, **57**, pp. 189–198

[5] He, D., Qiu, T., Luo, R.: 'Fuel efficiency-oriented platooning control of connected nonlinear vehicles: a distributed economic MPC approach', *Asian J. Control*, 2019, **21**, pp. 1–11

[6] Kamal, M., Mukai, M., Murata, J., *et al.*: 'Model predictive control of vehicles on urban roads for improved fuel economy', *IEEE Trans Control Syst Technol*, 2013, **21**, (3), pp. 831–841

[7] He, D., Shi, Y., Song, X.: 'Weight-free multi-objective predictive cruise control of autonomous vehicles in integrated perturbation analysis and sequential quadratic programming optimization framework', *J. Dyn. Syst. Meas. Contr.*, 2019, **141**, pp. 1–10

[8] Li, S.: 'Economy-oriented vehicle adaptive cruise control with coordinating multiple objective function', *Veh. Syst. Dyn.*, 2013, **51**, (1), pp. 1–17

[9] Li, S., Jia, Z., Li, K., *et al.*: 'Fast online computation of a model predictive controller and its application to fuel economy-oriented adaptive cruise control', *IEEE Trans. Intell. Transp. Syst.*, 2015, **16**, (3), pp. 1199–1209

[10] Cheng, S., Li, L., Mei, M.: 'Multiple-objective adaptive cruise system integrated with DYC', *IEEE Trans. Veh. Technol.*, 2019, **68**, (5), pp. 4550–4559

[11] Luo, L., Liu, H., Li, P., *et al.*: 'Model predictive control for adaptive cruise control with multi-objectives: comfort, fuel-economy, safety and car-following', *J. Zhejiang Univ.*, 2010, **11**, (3), pp. 191–201

[12] Luo, Y., Chen, T., Zhang, S., *et al.*: 'Intelligent hybrid electric ACC with coordinated control of tracking ability, fuel economy, and ride comfort', *IEEE Trans. Intell. Syst.*, 2015, **16**, (4), pp. 2303–2308

[13] Li, S., Cuo, Q., Xu, S., *et al.*: 'Performance enhanced predictive control for adaptive cruise control system considering road elevation information', *IEEE Trans. Intell. Veh.*, 2017, **2**, (3), pp. 150–160

[14] Zhu, M., Chen, H.: 'Vehicle adaptive cruise control strategy considering the time interval of workshop response', *J. Mech. Eng.*, 2017, **53**, (24), pp. 144–150

[15] Zhao, R.C., Wong, P., Xie, Z.: 'Real-time weighted multi-objective model predictive controller for adaptive cruise control systems', *Int. J. Autom. Technol.*, 2017, **18**, (2), pp. 279–292

[16] Mesbah, A.: 'Stochastic model predictive control: an overview and perspectives for future research', *IEEE Control Syst.*, 2016, **36**, (6), pp. 30–44

[17] Jing, J., Filev, D., Kurt, A.: 'Vehicle speed prediction using a cooperative method of fuzzy Markov model and auto-regressive model'. IEEE Intelligent Vehicles Symp., Los Angeles, CA, USA, 11–14 June 2017, pp. 881–886

[18] Bichi, M., Ripaccioli, G., Cairano, S., *et al.*: 'Stochastic model predictive control with driver behavior learning for improved powertrain control'. 49th IEEE Conf. on Decision and Control, Atlanta, GA, USA, 15–17 Dec. 2010, pp. 6077–6082

[19] Mcdonough, K., Kolmanovsky, I., Filev, D., *et al.*: 'Stochastic dynamic programming control policies for fuel efficient in-traffic driving'. Proc. of American Control Conf., Montréal, Canada, 27–29 June 2012, pp. 3986–3991

[20] Mozaffari, L., Mozaffari, A., Azad, N.: 'Vehicle speed prediction via a sliding-window time series analysis and an evolutionary least learning machine: a case study on San Francisco urban roads', *Eng. Sci. Technol.*, 2015, **18**, (2), pp. 881–886

[21] Stephane, L., Chao, S., Ruzena, B., *et al.*: '*Comparison of parametric and non-parametric approaches for vehicle speed prediction*'. Proc. of American Control Conf., Portland, OR, USA, 4–6 June 2014, pp. 3494–3499

[22] Rasmussen, C., Willams, C.: '*Gaussian processes for machine learning*' (MIT Press, Cambridge, MA, USA, 2006)

[23] Dominik, M., Roman, S., Harald, W., *et al.*: 'Flexible spacing adaptive cruise control using stochastic model predictive control', *IEEE Trans. Control Syst. Technol.*, 2018, **26**, (1), pp. 114–127

[24] Florian, M., Oliver, S.: 'An economic model predictive cruise controller for electric vehicles using Gaussian process prediction', *IFAC Papers Online*, 2018, **51**, (31), pp. 876–881

[25] Yulin, M., Zhi, X., Reza, M., *et al.*: 'Hierarchical fuzzy logic-based variable structure control for vehicles platooning', *IEEE Trans. Intell. Transp. Syst.*, 2019, **20**, (4), pp. 1–12

[26] Naranjo, J., Gonzalez, G., Garcia, R., *et al.*: 'Cooperative throttle and brake fuzzy control for ACC + stop & go maneuvers', *IEEE Trans. Veh. Technol.*, 2007, **56**, (4), pp. 1623–1630

[27] He, Z., Liu, G., Zhao, X., *et al.*: 'Review of Gaussian process regression', *Control Decis.*, 2013, **28**, (8), pp. 1121–1137

[28] Xiao, H., Liu, Y., Huang, D.: 'Application of Gaussian process modeling method in industrial process', *J. South China Univ. Technol.*, 2016, **44**, (12), pp. 36–43

[29] Malisani, P., Chaplais, F., Petit, N.: 'An interior penalty method for optimal control problems with state and input constraints of nonlinear systems', *Optim. Control Appl. Methods*, 2016, **37**, pp. 3–33

[30] Feller, C., Ebenbauer, C.: 'Relaxed logarithmic barrier function based model predictive control of linear systems', *IEEE Trans. Autom. Control*, 2017, **62**, (3), pp. 1223–1238

[31] Geneva, Switzerland, UNECE: '*Worldwide harmonized light vehicles test procedure*' (UNECE Global Technical Regulation, 2016). Available at: http://www.unece.org/fileadmin/dam/trans/doc/2016/wp29grpe/ECE-TRANS-WP29-GRPE-2016-03e_clean.pdf